

## THE EU FRAMEWORK V PROJECT “GEMCAR”: CEM TECHNIQUES INVESTIGATED

S. Alestra<sup>1</sup>, X. Ferrières<sup>2</sup>, J.P. Parmantier<sup>2</sup>, R. Perraud<sup>1</sup>, F. Rachidi<sup>3</sup>, A. Rubinstein<sup>3</sup>, A.R. Ruddle<sup>4</sup> and N. Whyman<sup>5</sup>

<sup>1</sup>EADS, Suresnes, France

<sup>2</sup>ONERA, Toulouse, France

<sup>3</sup>Swiss Federal Institute of Technology, Lausanne, Switzerland

<sup>4</sup>MIRA Ltd, Nuneaton, Warwickshire, UK

<sup>5</sup>QinetiQ, Farnborough, UK

(Principal contact: abraham.rubinstein@epfl.ch)

**Abstract:** This document provides a brief overview of the capabilities of the various numerical techniques that were adopted in the frame of the GEMCAR project, including a paralleized implementation of the widely used NEC2 “method of moments” code and a hybrid technique based on time-domain finite volume and finite difference codes.

### 1. Introduction

There is no single numerical method that meets all of the requirements for EMC modelling, with the result that it is necessary to deploy a range of tools to address specific aspects. Furthermore, there is no single technique from any specific class of tools that is uniquely suited to the solution of EMC related problems. Consequently, the purpose of this paper is to give a brief review of the types of numerical techniques that have been applied in the frame of GEMCAR project, the ways in which they can be used, and the relative merits and disadvantages of the numerical methods.

Details of the formulation of particular numerical techniques are not considered to be necessary in this document, as this information is readily available in the technical literature and is not of direct relevance to the issues considered here.

### 2. BEM coupled with cable network code – EADS

#### 2.1 Boundary element method code (ASERIS/BEM)

ASERIS/BE solves Maxwell’s equations in the frequency domain by a finite boundary element method (BEM). This code is widely used for EMC and antenna applications for complex geometries [1,2]. The quality of the expected results depends on the quality of meshing that is used. The size of the mesh elements should not be too large with respect to wavelength: one generally uses a rule of one-fifth of the wavelength  $\lambda$  (on average, the size of each edge of the meshing triangle will be  $h = \lambda/5$ ). This solver does not handle directly SDR Universal format files. A pre-processor analyses the electromagnetic complexity of the structure, and assigns to each of the element edges the number of degrees of freedom that are needed for the unknowns that are required to solve Maxwell’s equations.

For surface elements, these unknowns are the electric and magnetic current fluxes of induced currents across the mesh edges. They are located at the middle of the sides of triangles.

For a given frequency, the code assembles one matrix, factorizes it, and then solves a linear system with the right hand side containing the illumination distribution. A frequency value or a frequency range and a step are set for the calculation. The main limitation of these techniques is in the memory requirement, because a dense matrix describing the interactions between the different cells has to be stored.

Electromagnetic fields are calculated in the vicinity of the structures at particular points defined by the user. Calculation of the scattered field is obtained by subtracting the incident field from the total field. The scattered field at any point in a homogeneous domain is expressed by a surface integral on the boundary of that domain. For a perfect conductive object, this expression depends on the surface electric currents through an integral-differential operator.

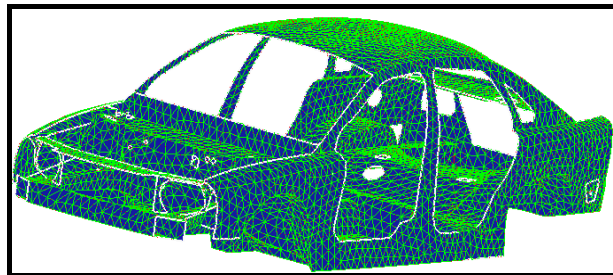


Fig. 1: BEM mesh for simplified bodyshell

#### 2.2 Cable network code (ASERIS/NET)

The 3D Finite Boundary Element code can be used to compute the incident field on a wiring, the response of the wiring being solved with a cable network code. The method theoretically comes from the “field-to-transmission-line” model. In this model, the incident field is transformed into equivalent generators, driving currents on the wiring. In this approach, it is important to understand that “incident” field means the field in the absence of the wiring. Therefore, the 3D incident field calculation does not require the wires to be meshed, which may be seen as a great advantage.

Three equivalent field-to-transmission line models are available (Taylor et al. [3], Agrawal et al. [4], and Rachidi [5]). ASERIS/NET is based on Taylor’s model, in which the coupling of an incident field on a cable is equivalent to applying a set of distributed current and voltage generators, expressed in terms of the incident electric and magnetic fields [3].

ASERIS-NET simulates the interference on an electrical or electronic network, resulting from local injections and distributed sources, due to natural or artificial external ambient fields or electromagnetic disturbances. The distributed field sources are computed by the 3D code and are coupled on the cables by solving the transmission line equations in the frequency range of interest.

Multiconductor transmission lines are convenient models to describe at the same time EM coupling and propagation on cable bundles. We refer to the BLT equation formulated on cable networks [6], and also on study the transmission line models at high frequencies using a rough, non-uniform description [7].

Input parameters for the simulations described above include the bundle construction (single conductor wire), electrical characterization (RLCG matrices), the various geometrical shapes of the bundles, shield or non-shield and integration of dielectrics in the wires, the loads or devices: linear circuits (R, L and C). Outputs from the simulations are frequency domain currents and voltages at any point of the network. Scattering parameters between the network ports can also be computed from these currents and voltages. The scattering matrices “S”, referenced to the characteristic impedance of the tubes connected in the network, have a physical significance in terms of the network transmission and reflection coefficients [8].

### 3. Method of moments (MoM) – EPFL

In the framework of the GEMCAR project, EPFL uses the Numerical Electromagnetics Code (NEC), a freely distributed incarnation of the MoM. The NEC code is a user-oriented software tool for analyzing the electromagnetic response of antennas and other metal structures [9]. In the last 20 years, NEC has been widely and successfully applied to radio communications testing as well as antenna design. As the code is written in FORTRAN, it is readily compiled and run on a variety of platforms featuring all kinds of operating systems, an advantage of the portability of the language.

Since NEC uses models represented by means of wires, the numerical core allows the simulation of very complex 3D structures, limited only by the capacity of the environment in which it runs, with memory as the main constraint. The NEC code produces an interaction matrix representing the system of integral equations that leads to the calculation of the currents and consequently the fields. The dimension of this matrix depends on the number of segments that are needed in the model to represent the structure to be evaluated. The matrix is then reduced using LU factorization and, with the aid of the excitation vector, the final solution to the integral equations is obtained [10].

For a model consisting of  $N$  segments, the amount of memory required by NEC is proportional to  $N^2$ . As a consequence of the square growth in the expression, the amount of memory required becomes important on many current computers at around 3000 segments. An ‘out-of-core’ routine is embedded into NEC to allow the use of the hard disk as swap memory in case of bigger models. The matrix is cut in pieces that are stored on the hard disk, following a special pattern. The operating system can then use all available RAM and NEC manages the disk swapping. The out-of-core routine requires about four times the normal RAM and, as a consequence, enormous swap files are created. Even more important is the fact that the use of the hard disk, through the swap file, will slow down the execution of NEC to unpredictable values.

In order to overcome this problem, the only solution seems to be more memory. Having as much memory as needed is the best way to assure an optimal execution. However operating systems are not capable of managing all the memory one would be prepared to buy. There are limits imposed by the operating systems to the size of an executable application. Thus, a version of NEC compiled for a very large number of segments will fail to start, because operating systems are unable to allocate enough memory for the declared matrix sizes.

#### 3.1 Parallel NEC [11, 12]

The original NEC code can be globally divided in two parts:

- (1) The input section, which reads geometrical information about the model and stores the “cards” that dictate additional model information, program commands and execution requirements.
- (2) The calculation section, which computes the coefficients of  $[G]$  for the matrix equation  $[G][I]=[E]$  and solves this equation by means of the Gauss-Doolittle numerical method. This method solves the system by first calculating the LU decomposition of  $[G]$  into  $[L]$  and  $[U]$  so that the matrix equation becomes  $[L][U][I]=[E]$ . The equation is solved by forward substitution in  $[L][F]=[E]$  and backward substitution in  $[U][I]=[F]$  so that the  $[I]$  vector containing the currents for every single segment is obtained.

The major computational effort is factoring  $[G]$  into  $[L]$  and  $[U]$ . In fact, computation of the elements of the matrix  $[G]$  and the solution of the matrix equation are the two most time-consuming steps in computing the response of a structure, often accounting for over 90% of the computation time [9]

Since the NEC code is open and freely available, we have been able to modify it and include a certain number of routines so that the program can also be executed in parallel supercomputing architectures. The idea behind this technique is to share the interaction matrix among a number of processor ( $P$ ) so that the memory requirements can be fulfilled and the total computing power help produce faster results.

The routine that computes the elements of the interaction matrix was substituted by algorithms that partition the matrix assign to each processor the task of calculating only those elements that belong to its local sub-matrix. In this way, we reduce the per-processor memory requirements by nearly a factor of  $P$ , for a machine with  $P$  processors. The factorization and solution routines were substituted by highly optimized scalable parallel solvers that deliver dramatic improvements in execution times, particularly for cases where disk swapping is unavoidable on single processor machines. Representative timing and memory results (based on a test model) are shown in Table 1 below. These results compare both the both original version of NEC on a single PC and the modified version on a parallel supercomputer.

Special care must be taken when building a complex NEC model. In addition to a series of basic guidelines for the simulation of antennas and other single structures [9], other considerations, derived primarily from empirical observations, are of considerable importance for surface simulations. In particular, a model of very high geometrical complexity, from the visual point of view, does not necessarily guarantee better results than can be obtained from a model based on a much simpler representation of the geometry.

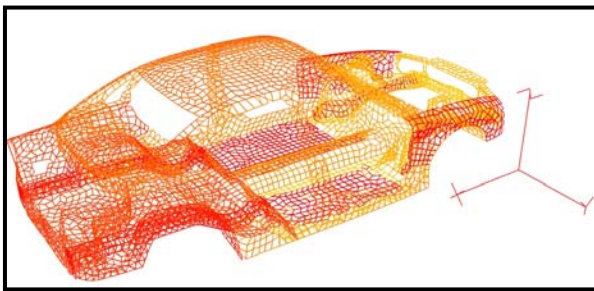
**Table 1:** Timing and memory as a function of the number of processors for a 6753 segments test case.

Number of Processors	Matrix Filling Time	Matrix Factorization Time	Run Time (for 2 frequencies)	Memory per processor (MB)	Total Memory (MB)
1 – PC	10 min	6 h 47 min	14 h 6 min	62*	2790
4 – T1	2 min 56 sec	5 min 24 sec	16 min 7 sec	193.9	769.34
8 – T1	2 min 42 sec	2 min 45 sec	11 min 37 sec	104.4	816.04
16 – T1	2 min 34 sec	1 min 31 sec	8 min 52 sec	57.28	883.76
24 – T1	2 min 50 sec	1 min 39 sec	8 min 29 sec	39.55	905.81
32 – T1	2 min 33 sec	1 min 27 sec	8 min 16 sec	33.72	1019.45
36 – T1	3 min	1 min 3 sec	8 min 34 sec	28.45	988.57

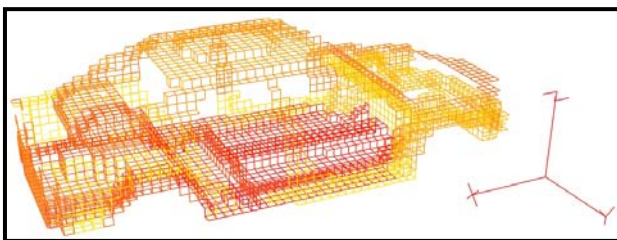
\*Approximation based on core storage of 2000 segments.

### 3.2 MoM meshing issues

Two different approaches for the meshing of the GEMCAR simple test case model are shown in Fig. 2, for example, both converted into NEC input files. It was observed that the more accurate body-fitted model (a) produced satisfactory results of a very narrow frequency interval. However, the stair-cased approximation (b) produced a very good agreement for a wide interval and for different configurations of the experiment.



(a) Body fitted mesh



(b) Stair-cased approximation (derived from TLM model)

**Fig. 2:** Two different approaches for the NEC mesh

The most important parameter that determines the accuracy of the results appears to be the wire radius. The guidelines stated in [9] for the representation of segment lengths and radius do not apply in an identical manner in the case of wire-grid surface simulations. The so-called “equal area rule” [12], has been shown to give the best results when it comes to perfectly square and homogeneous meshes. In fact, the application of the rule is also a guarantee that some of the other guidelines regarding the use of NEC are respected. For example, a completely square and homogeneous mesh will ensure that all segments have the same length and radius, a condition that is highly desirable for successfully modeling complex 3D surfaces with NEC.

On the other hand, the extension of the application of the equal area rule to more complex, body-fitted meshing techniques (i.e. with a triangular mesh) does not provide the same degree of accuracy, possibly due to the fact that significant variations in segment length and radius result.

### 4. Transmission line matrix (TLM) – MIRA

The transmission line matrix (TLM) method [13,14] is a full-wave, 3D electromagnetic field modelling technique. In this approach, the entire volume is discretized using structured hexahedral cells (usually rectangular, but sometimes cylindrical) that are occupied by a “node” connecting 12 transmission lines, representing two orthogonal polarizations at each of the cell faces. Boundary conditions are applied by appropriate termination of the transmission lines, while materials are represented by adding stubs to the node to modify the propagation characteristics. Like FDTD, TLM is attractive for EMC applications because it is normally formulated in the time-domain, thus permitting broadband frequency-domain results to be obtained from Fourier transformation of a single time-domain response.

As TLM employs a structured mesh, very large models can be accommodated within relatively modest computing resources. Furthermore, sub-cell models are available for long, thin features, thus ensuring that common elements such as wires [15] (including multi-conductor bundles [16]) and slots [17] can also be efficiently represented in models of large structures. Frequency dependent materials [18,19] and features such as arrays of apertures [20] can also be accommodated using special models.

In common with other finite methods, such as FDTD and finite elements, the modeled volume must be truncated with an artificial absorbing boundary. In TLM this can be achieved by using simple matched (ie.  $377 \Omega$ ) terminations at free space boundaries that are sufficiently far from the radiating or scattering structures, or with more sophisticated PML schemes. The main disadvantages of TLM, like FDTD, are its inability to provide a body-fitted mesh for arbitrary geometries (with the result that curves are normally represented by a staircased approximation) and the fact that the duration of simulations for highly resonant structures can be very long. However, these issues are not found to be serious limitations in most automotive EMC modeling applications.

A sample vehicle TLM mesh is illustrated in Fig. 4, for a bodysell containing a simple wiring harness and illuminated by a nearby antenna. Thus, the harness model in this case is fully integrated with the 3D electromagnetic model.

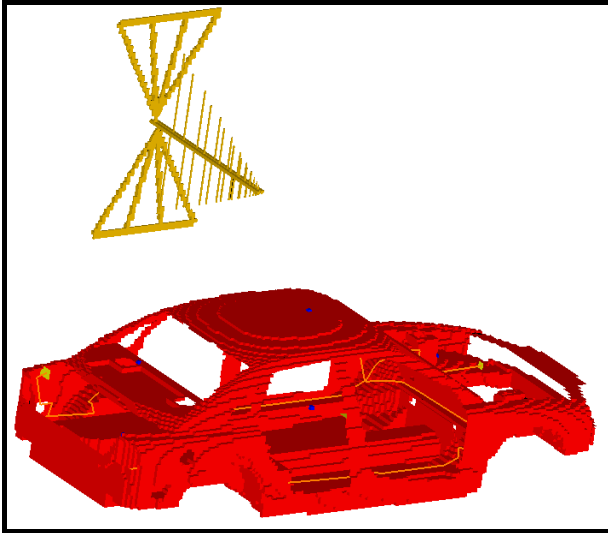


**Fig. 3:** TLM mesh for simplified bodyshell, with integrated harness model and vertical biconilog antenna at side

This capability is needed for areas where the cables are a significant distance from the bodyshell (typically in the dashboard area and engine bay). However, for those parts of the harness that are close to the bodyshell a separated method would avoid the the need to allow for the long “ringing” times that result from adding additional resonances associated with the cables to the 3D model.

## 5. FDTD – ONERA and QINETIQ

The method used is based on the well-known Yee scheme [21], where the Maxwell equations are solved in time domain and in a bounded computational space domain. The boundaries of the computational domain taken into account, permit to simulate the infinite space with Berenger’s PML formalism [22] or a special condition such as a conducting plane to simulate, for example, the ground plane in the MIRA and EPFL measurements for the GEMCAR project.

In the Yee scheme, the computational domain is split into a grid of parallelepipedic cells where different spatial steps are given in the three directions ( $x$ ,  $y$  and  $z$ ). The unknowns of the method are the electric and magnetic field components. The electric field components ( $E_x$ ,  $E_y$  and  $E_z$ ) are located in space at the edges of the cells of the grid. For the magnetic fields a second grid (“dual grid”) is defined, the vertices of which are located at the centers of the cells of the first grid. The magnetic field components ( $H_x$ ,  $H_y$  and  $H_z$ ) are then located at the edges of this dual grid (see Fig. 4 below).

The magnetic and electric fields are not located at the same position in space: the numerical scheme is described as “leap-frogged” in space. In this method, the electric and magnetic fields are evaluated with a delay of  $dt/2$  where  $dt$  represents time step. The scheme is also leap-frogged in time. This leap-frog approach permits an explicit second-order numerical method with a Courant Frederick Levy (CFL) condition of:

$$dt < \frac{1}{c} \left( \frac{1}{dx^2} + \frac{1}{dy^2} + \frac{1}{dz^2} \right)^{-1/2}$$

where  $c$ ,  $dt$ ,  $dx$ ,  $dy$  and  $dz$  define respectively the speed of light, the time step and the spatial step size along the three orthogonal axes.

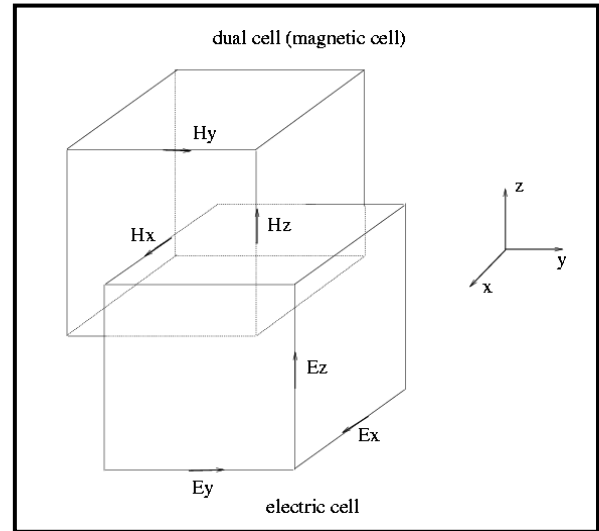


**Fig. 4:** Locations of unknowns in the FDTD method

The choice of this numerical approach results in a stair-cased representation of objects with surfaces that are not aligned with the mesh. An example of an FDTD mesh is illustrated in Fig. 5, for the MIRA test case simulation.

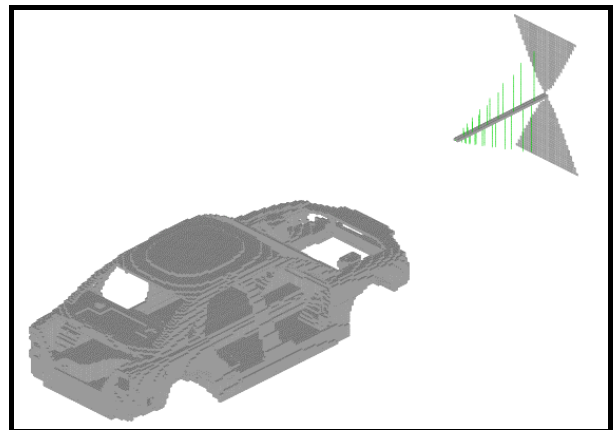


**Fig. 5:** ONERA FDTD mesh for a MIRA test configuration

A special wire model formalism due to Holland and Simpson [23] can be used to take account of thin wires in FDTD models without meshing them in fine detail, which adversely impact on both the memory requirements and runtime of FDTD models. The wire is represented using a sequence of broken lines that follow the edges of the electric grid with appropriate boundary conditions at its two terminations (eg. wire open circuit or connected to metal).

In conclusion, the method is robust and very attractive in term of CPU time. However, in order to compute a field at a given position, the field components along the cell edges must be interpolated in order to obtain the field at specific points inside the cells. This can be a disadvantage when the fields along a path close to an object are required.

## 6. Hybrid FDTD/FVTD method – ONERA

The hybrid technique used by ONERA combines the finite difference (FDTD) and finite volume (FVTD) methods to solve the Maxwell’s equations in the time domain.

This method, developed at ONERA and implemented in the code EIVE, combines two kinds of meshes and two different numerical schemes:

- (1) The first is the well-known FDTD method based on the Yee scheme [21]. This scheme is applied only on a structured Cartesian mesh where the size of the cells can be different on each axis and along a given axis. In this case a perfectly matched layer (PML, [22, 24] is used to truncate the computational domain.
- (2) The second is a cell-centered finite volume scheme that solves a conservative form of Maxwell's equations [25]. In this method the computational domain is split into a set of non-structured cells, which can be cubic, pyramidal, tetrahedral, prism, etc. The magnetic and electric fields are located at the center of the cells. The computational domain is bounded by a Silver Muller condition to simulate infinite space.

The code EIVE offers the possibility to use only the FDTD method, only the FVTD method, or both methods simultaneously. In the latter possibility, the mesh over the computational domain is composed of a structured zone, where the FDTD scheme is applied, and an unstructured zone where the FVTD scheme is applied. The hybridization between the two schemes is achieved using one or more overlapping cells, where the fields at the time  $t+dt$  are computed for each method by using the fields at the time  $t$  evaluated by the other method [26]. The CFL number for the two methods is not the same and the CFL number for the FVTD scheme implies generally a much smaller time step than the FDTD scheme.

This is due in part to the numerical scheme but also to the size of the cells that are used, which are generally smaller in the unstructured part than in the structured part of the mesh. To avoid the situation where the smallest cells in the unstructured part impose the overall time step for the hybrid method, a local time step is used to evaluate the fields inside these cells. Fields in the others cells are computed with time steps corresponding to the FDTD CFL number for the structured part and to the FVTD CFL number for the unstructured part.

In the GEMCAR model, the antennas and the computational domain is defined using a structured mesh except in the vicinity of the car where an unstructured, body-fitted mesh is used (see Fig. 6).

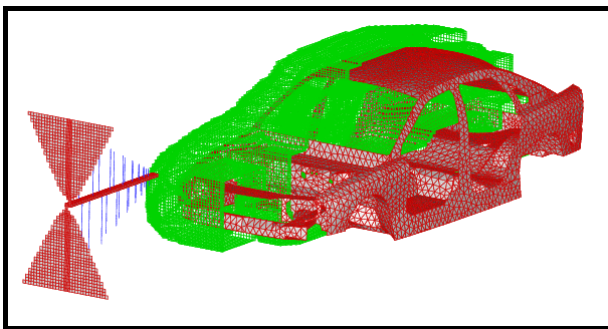


**Fig. 6:** Hybrid FV/FDTD mesh showing the boundary between the structured and unstructured parts.

We consider that the antenna is sufficiently Cartesian to be meshed with a structured mesh. Near the bodyshell, however, the mesh is composed of unstructured tetrahedral cells derived from a body-fitted surface mesh based on triangular elements.

In particular, this condition is important to evaluate the electric fields tangential to the path of the harness inside the car.

The hybrid method offers a compromise between a fast method based on a stair-cased model (FDTD), which needs a very fine mesh to correctly capture the path of the harness, and an entirely conformal method (FVTD) which implies too large a number of unstructured cells in order to correctly model the antenna geometry, resulting in requirements for much greater memory and CPU time than FDTD.

## 7. Conclusions

The range of different numerical techniques that are represented in the GEMCAR project is representative of the currently available electromagnetic modeling techniques, but not complete. Nonetheless, the techniques that are described here are probably the most widely used techniques for EMC applications, particularly for modeling electrically large structures over a wide range of frequencies.

## 8. Acknowledgments

This work was carried out as part of the GEMCAR project, a collaborative research project supported by the European Commission under the competitive and Sustainable Growth Programme of Framework V (EC contract G3RD-CT-1999-00024) and by the Swiss Federal Office for Education and Science (Grant No. 99.0377).

The project consortium includes MIRA Ltd (coordinator), QinetiQ and Ford Motor Company Ltd of the UK, EADS CCR, CETIM and ONERA of France, EPFL (Switzerland), Hexrox EMC and Safety Services NV/SA (Belgium) and Volvo TDC (Sweden).

The consortium also acknowledges the support of Volvo Cars (Sweden) in providing vehicles and CAD data for use within the GEMCAR project.

## 9. References

- [1] G. Alléon, S. Amram, N. Durante, P. Homsy, D. Pogarielloff and C. Farhat, "Massively parallel processing boosts the solution of industrial electromagnetic problems: high performance out-of-core solution of complex dense systems", *Proceedings of the 8<sup>th</sup> SIAM Conference on Parallel Processing for Scientific Computing*, 1997
- [2] G. Alléon, M. Benzi, and L. Giraud, "Sparse approximate inverse pre-conditioning for dense linear systems arising in computational electromagnetics", Technical Report TR\_PA\_97\_05, CERFACS, 1997
- [3] C.D. Taylor, R.S. Satterwhite and C.W. Harrison, "The response of a terminated two-wire transmission line excited by a non-uniform electromagnetic field", *IEEE Transactions on Antennas and Propagation*, Vol. 13, No. 6, November 1986, pp. 987-989
- [4] A.K. Agrawal, H.J. Price and S.H. Gurbaxani, "Transient response of multiconductor transmission lines excited by a non-uniform electromagnetic field", *IEEE Transactions on Electromagnetic Compatibility*, Vol. 22, No. 2, May 1980, pp. 119-129
- [5] F. Rachidi, "formulation of field to transmission line coupling equations in terms of magnetic excitation field", *IEEE Transactions on Electromagnetic Compatibility*, Vol. 35, No. 3, August 1993 pp. 403-407

- [6] C.E. Baum, T.K. Liu and F.M. Tesche, "On the analysis of general multiconductor transmission-line networks, electromagnetic topology for the analysis and design of complex systems", in J.E. Thompson and L. H. Heussen (eds.), *Fast Electrical and Optical Measurements*, Martinus Nijhoff, Dordrecht, 1986 pp. 467-547
- [7] J.P. Parmantier, V. Gobin, F. Issac, I. Junqua, Y. Daudy, and J.M. Lagarde, "An Application of the Electromagnetic Topology Theory on the Test-bed Aircraft", EMPTAC, *Interaction Notes*, Note 506, November 1993.
- [8] J.P. Parmantier, S. Bertuol, X. Ferrières and C.E. Baum, "Optimisation of the BLT equation based on a sparse Gaussian elimination", *Proceedings of 13<sup>th</sup> International Zurich EMC Symposium*, Zurich, Switzerland, February 1999, pp. 137-142
- [9] G. Burke and A. Poggio, "Numerical electromagnetics code - method of moments", Livermore National Laboratory, Livermore, CA, Lawrence Report No. UCID-18834, 1981.
- [10] A. Rubinstein, F. Rachidi and M. Rubinstein, "Development of an optimized parallel Numerical Electromagnetics Code (NEC) and its implementation on the Swiss-T1 and Eridan parallel supercomputers", *Applied Computational Electromagnetics Society Conference ACES*, March 2001, Monterey, California.
- [11] A. Rubinstein, F. Rachidi, M. Rubinstein and B. Reusser, "Electromagnetic Analysis of Large Structures Using the Method of Moments", Paper submitted to *IEEE Transactions on EMC*, 2002
- [12] E.K. Miller, "PCs and AP and Other EM Reflections", *IEEE Antennas and Propagation Magazine*, Vol. 39, No. 1, Feb 1997
- [13] P.B. Jones, "A symmetrical condensed node for the TLM method", *IEEE Transactions on Microwave Theory and Techniques*, Vol. 33, No. 10, 1985, pp. 882-992
- [14] W.J.R. Hofer, "The transmission-line matrix method: theory and applications", *IEEE Transactions on Microwave Theory and Techniques*, Vol. 33, No. 10, 1985, pp. 882-892
- [15] A.J. Wlodarczyk and D.P. Johns, "New wire interface for graded 3-D TLM", *Electronics Letters*, Vol. 28, No. 8, pp. 728-729
- [16] A.J. Wlodarczyk, V. Trenkic, R.A. Scaramuzza and C. Christopoulos, "A fully integrated multiconductor model for TLM", *IEEE Transactions on Microwave Theory and Techniques*, Vol. 46, No. 12, December 1998, pp. 2431-2437
- [17] V. Trenkic and R.A. Scaramuzza, "Modelling of arbitrary slot structures using transmission line matrix (TLM) method", *Proceedings of 14<sup>th</sup> International Zurich EMC Symposium*, Zurich, Switzerland, February 2001, pp. 393-396
- [18] J.F. Dawson, Representing ferrite absorbing tiles as frequency dependent boundaries in TLM, *Electronics Letters*, Vol. 29, No.9, April 1993, pp.791-792
- [19] J. Paul, C. Christopoulos and D.W.P. Thomas, "Generalized material models in TLM—Part 1: Materials with frequency dependent properties", *IEEE Transactions on Antennas and Propagation*, Vol. 47, October 1999, pp. 1528-1534
- [20] N. Doncov, J. Wlodarczyk, R. Scaramuzza and V. Trenkic, "Modelling of airflow aperture arrays using the transmission line matrix (TLM) method", *Proceedings of 15<sup>th</sup> International Zurich EMC Symposium*, Zurich, Switzerland, February 2003
- [21] K.S.Yee, "Numerical solution of initial boundary value problems involving Maxwell's equations in isotopic media", *IEEE Transactions on Antennas and Propagation*, Vol. AP-14, May 1966, pp. 302-307
- [22] J.P. Berenger, "A perfectly matched layer for the absorption of electromagnetic waves," *Journal of Computational Physics*, Vol. 114, pp. 185-200, 1994.
- [23] P. Holland and L. Simpson, "Finite difference analysis of EMP coupling to thin struts and wires", *IEEE Transactions on Electromagnetic Compatibility*, Vol. 23, May 1981, pp. 89-99
- [24] S. Gedney, "An anisotropic perfectly matched layer-absorbing medium for the truncation of FDTD lattices," *IEEE Transactions on Antennas and Propagation*, Vol. 44, No. 12, December 1996, pp. 1630-1639
- [25] P. Bonnet, X. Ferrières, F. Issac, F. Paladian, J. Grando, J.C. Alliot and J. Fontaine, "Numerical Modeling of scattering problem using a time domain finite volume method", *JEWA*, Vol. 11, pp. 1165-1185, 1997
- [26] X. Ferrières, J.P. Parmantier and S. Bertuol, "Méthode hybride couplée à une équation de réseau pour le calcul des perturbations induites sur le câblage d'une voiture", *Actes du Colloque CEM 2002*, Grenoble, March 2002